JTTEE 2:59-68

Characteristics and Corrosion Performance of 80Ni-20Cr Coating Deposited by On-Site Thermal Spraying

M. Takemoto and G. Ueno

New controlled atmosphere on-site spraying systems were developed to deposit a high-quality coating with superior resistance to wet corrosion. Characteristics and corrosion resistance of coatings deposited by arc and flame spraying of wire in argon gas were compared with those of coatings deposited by conventional and low-pressure plasma techniques. It was found that the coating deposited by the arc spraying of wire in argon gas is free of oxides and possesses excellent corrosion resistance in chloride and acid solutions. The coating suffers slight pitting and crevice corrosion associated with the isolated pores and electric potential paths. Corrosion resistance was improved by using a modified spraying system.

1. Introduction

THERMAL spraying of alloys has been widely used in Japan for on-site repair and upgrading of degraded process equipment.[1-3] Thermal spraying of aluminum and aluminum-zinc alloys is known to provide excellent corrosion protection to steel. The corrosion protection mechanism is by sacrificial anodic behavior of the active aluminum and aluminum-zinc.[4]

To combat excessive wet corrosion, the coating deposited by thermal spraying must isolate the substrate steel from aggressive environments because corrosion resistance is conferred by the passivation of the alloy. Coatings deposited by flame or arc spraying in air (conventional spraying) contain a number of pores, oxides, unmelted particles, and sometimes connected paths (i.e., permeable networks) through the coating. Thus, the corrosion resistance of the sprayed coating is usually very poor in the as-sprayed condition.[5] Corrosion resistance of sprayed porous coatings can be improved by artificial sealing with organic compounds or by self-sealing of the coating during service.

To convert a porous coating to a dense coating, or to produce an alloyed layer, post-spray heat treatment, laser glazing and alloying, and hot isostatic pressing (HIP) treatment have been attempted.[5-7] Successful field applications have not been reported because of limited application of these technologies to on-site construction equipment. Thermal damage due to excessive heating of substrate materials induced by post-spray treatment is also a problem in most construction materials. Thermal spraying possesses an advantage in producing coatings on-site without inducing significant thermal damage that would alter the prime function of the structure.

To endow low-grade construction material with the corrosion resistance of alloyed materials by on-site spraying, two types of portable spraying systems that operate in a controlled inert gas have been developed. This article discusses the characteristics and corrosion-resistance of 80Ni-20Cr coatings and compares performance with that of coatings deposited by conventional and low-pressure plasma spraying. Coatings glazed by a carbon dioxide laser were also tested.

Keywords: arc spraying, corrosion resistance, flame spraying, laser glazing, shrouded spraying

M. Takemoto, Professor, Aoyama Gakuin University, College of Science and Engineering, Dept. of Mechanical Engineering, Tokyo, Japan; and **G. Ueno,** President, Kanmeta Engineering Co. Ltd., Osaka, Japan.

2. Specimens and Experimental Methods

Coatings deposited on carbon steel by five spraying systems were tested. These systems were acetylene-oxygen flame spraying of wire in air (Type A), DC arc spraying of wire in air (Type B), flame spraying of wire in argon gas (Type C), arc spraying of wire in argon gas (Type D), and low-pressure plasma spraying (Type E). Types A and B coatings were deposited by conventional spraying, and Types C and D coatings were deposited by spraying in argon gas. Figure 1 shows a schematic of the spraying gun for DC arc and flame spraying under an argon gas to minimize the oxidation of fused metal. Argon was used as both a primary gas to accelerate fused particles and as a secondary controlling atmosphere gas. This portable gun makes it possible to accomplish on-site spraying. The edges of a structure can also be

Table 1 Chemical composition of spraying wire

Wire/powder	Composition, % Ni	Cr	C	Si	Mn	P	S	Fe
1.6-mm wire for arc spraying	77.83	20.47	0.03	1.28	0.01	0.001	0.001	0.10
3.2-mm wire for flame spraying	77.83	20.47	0.03	1.28	0.01	0.001	0.001	...
Powder for low-pressure plasma spraying	78.12	19.53	0.014	1.46	0.86	...	...	...

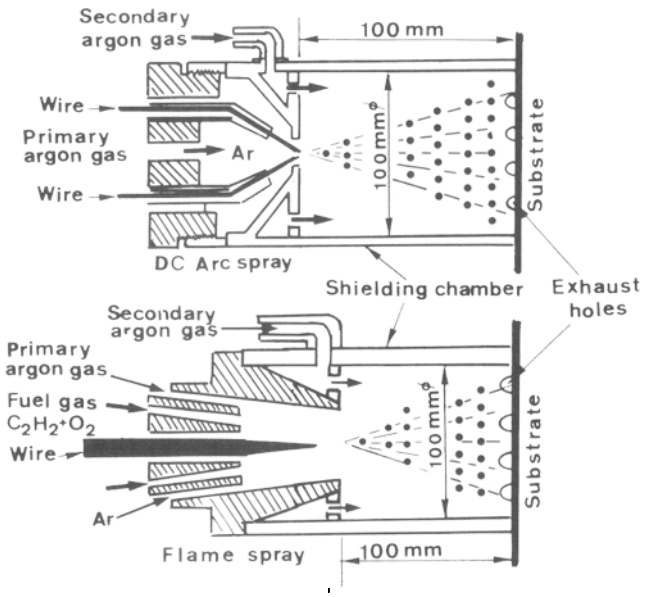

Fig. 1 Schematic of modified spraying guns for DC arc and flame spraying using an argon shroud.

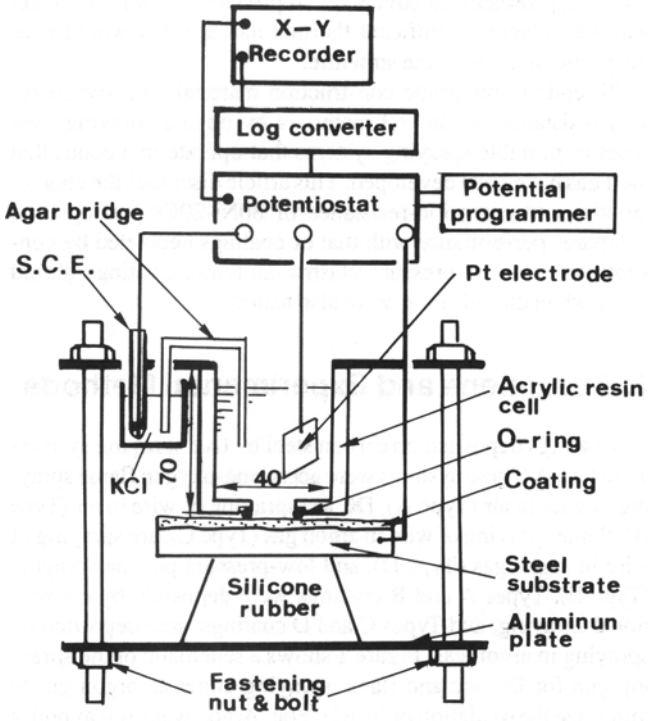

Fig. 2 Corrosion cell for measuring the polarization curves of coated steel.

sprayed by using a shielding chamber that is grooved. The wire diameter for the flame (Metco 12 E gun) and arc spraying (Metco 4RG gun) was 3.2 and 1.6 mm, respectively. The chemical composition of these materials is shown in Table 1.

Alloy powder of about 60 μm diameter was used for low-pressure plasma spraying. Low-pressure plasma spraying (LPPS) was performed at 100 torr in argon gas using argon-

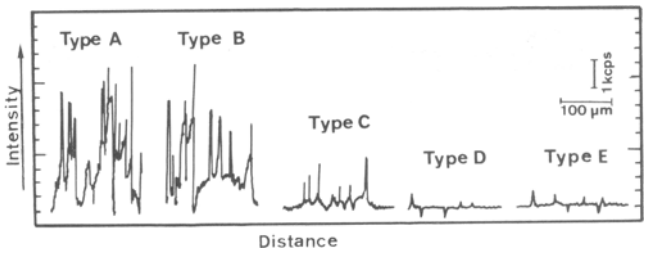

Fig. 3 Comparison of characteristic X-ray profiles of oxygen in coatings deposited by various thermal spraying processes.

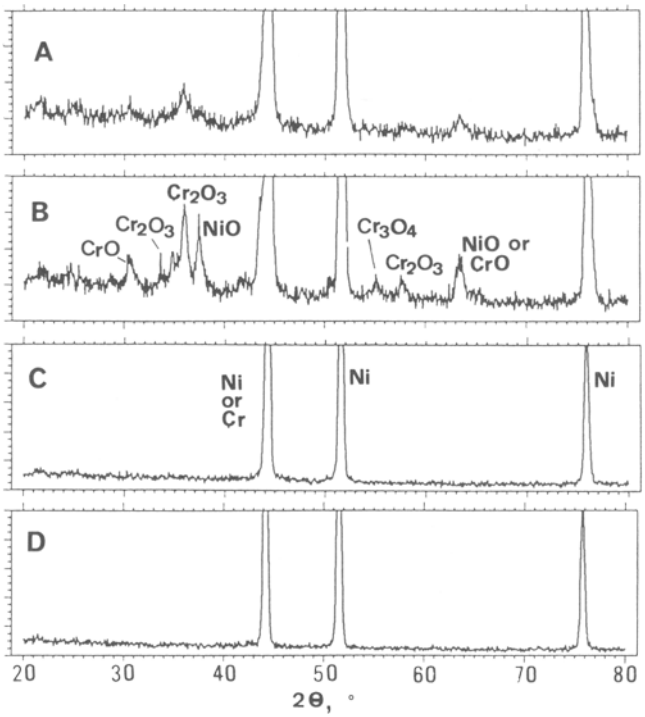

Fig. 4 X-ray diffraction patterns of coatings deposited by thermal spraying.

helium plasma gas at 30 V and 400 A. The LPPS process could not be performed on-site, and the coupons were prepared so that comparative corrosion studies could be performed. The oxygen concentration of the spray atmosphere decreases in the order of Type A, B, C, D, and E.

The chemical composition of the metallic phase of the sprayed coatings changes greatly depending on the spraying method. For instance, chromium in the spraying wire is converted to chromium oxide, and therefore, the chromium concentration in the metallic phase decreases. The compositional change in the coatings was examined by the electron probe microanalysis (EPMA). Because the concentration in Types A and B could not be determined correctly due to extremely large fluctuations, thin surfaces of these coatings were laser fused in argon gas to obtain a homogeneous metallic phase so that diffusion of iron and further oxidation could be avoided.[8]

Corrosion resistance of the coatings was compared with that of the constituent plate by measuring the potentiostatic polarization curves at a sweep rate of 1 mV/s. Polarization curves were

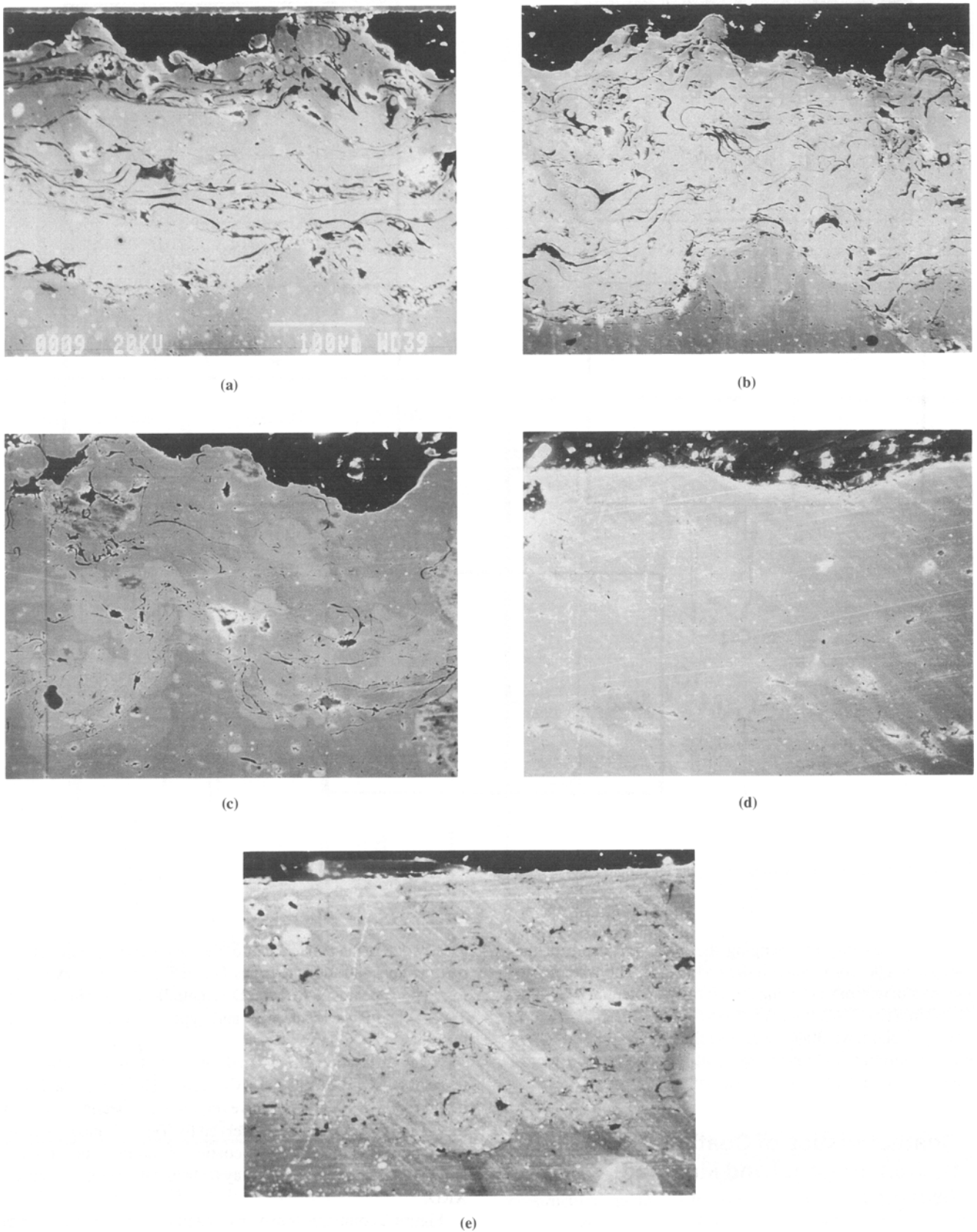

Fig. 5 Transverse microphotograph of coatings deposited by thermal spraying.

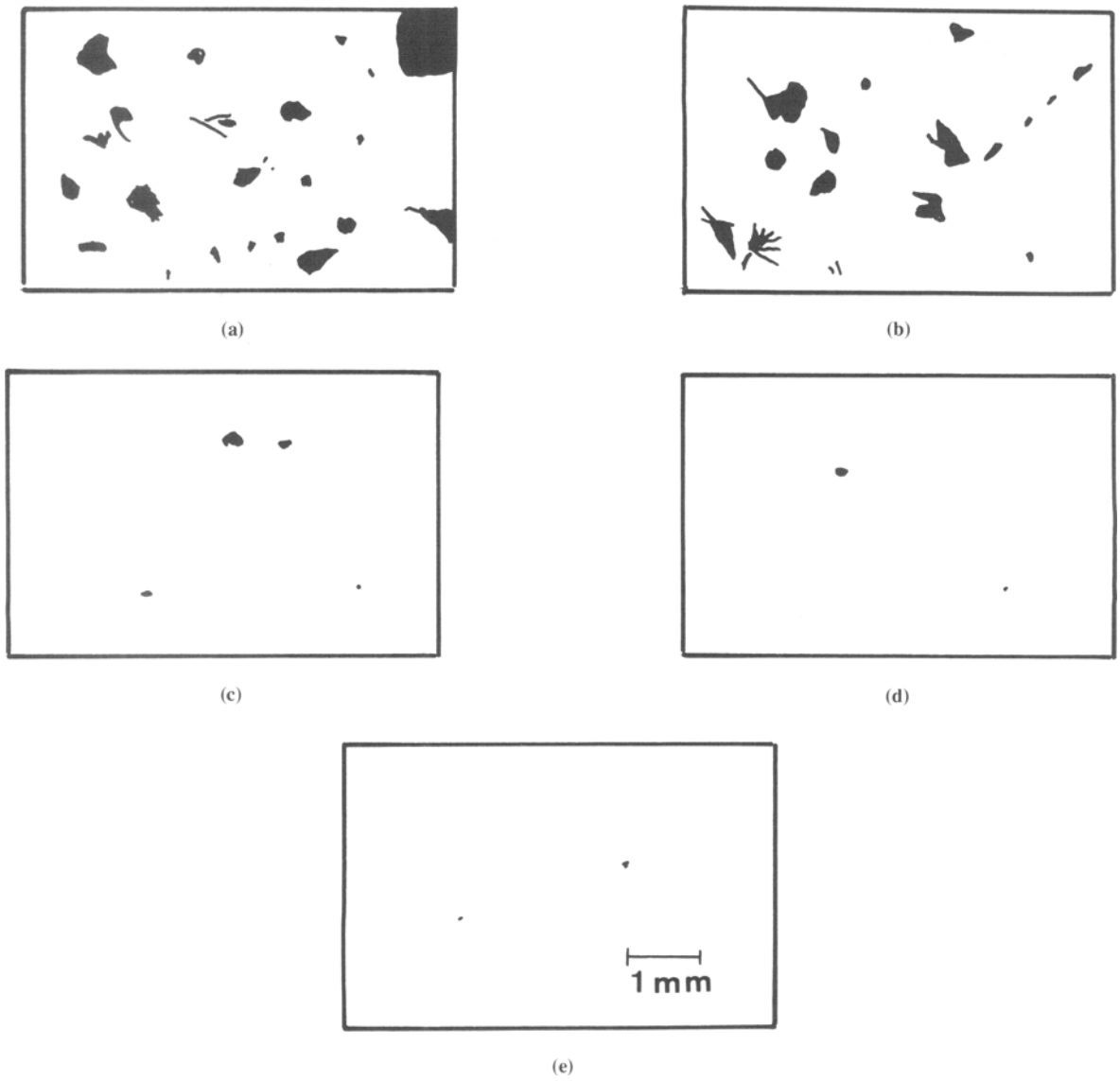

Fig. 6 Distribution of iron-ferricyanide spots for various types of coatings.

measured repeatedly by changing the place and depth of the coating using the corrosion cell shown in Fig. 2. The system consisted of a potentiostat (Nichia NP-IR1000), potential programmer (Nichia ES-51A), log converter (Nichia 100P), and an *X-Y* recorder (Yokogawa 3086). Because the cell is attached to the specimen through an O-ring, this configuration permits measurement of crevice corrosion resistance.

3. Characteristics of Coatings Deposited by Conventional and Modified Spraying

Oxygen concentrations (characteristic X-ray intensity by EPMA) in the coatings are compared in Fig. 3. The concentration of oxygen in Types A and B coatings is high and fluctuates greatly due to the existence of oxides and pores. In contrast, the oxygen concentration in Types D and E coatings is extremely low. The appearance of Type D is metallic and bright, whereas Types A and B are black-gray, and Types C and E are light gray in color.

X-ray diffraction (XRD) analyses (Fig. 4) revealed the existence of NiO, CrO, Cr_2O_3, and Cr_3O_4 as well as nickel and chromium for Types A and B. However, only the metallic phases of nickel and chromium were observed for Types C and D. The absence of oxides in the Type C coating is contradictory to Fig. 3 and suggests that any oxides may be below the detection limit of XRD.

Figure 5 compares transverse scanning electron microscope (SEM) photographs of coatings deposited by thermal spraying. Types A and B contain a number of elongated oxides and pores. In contrast, the structure of Type D is very dense and almost free

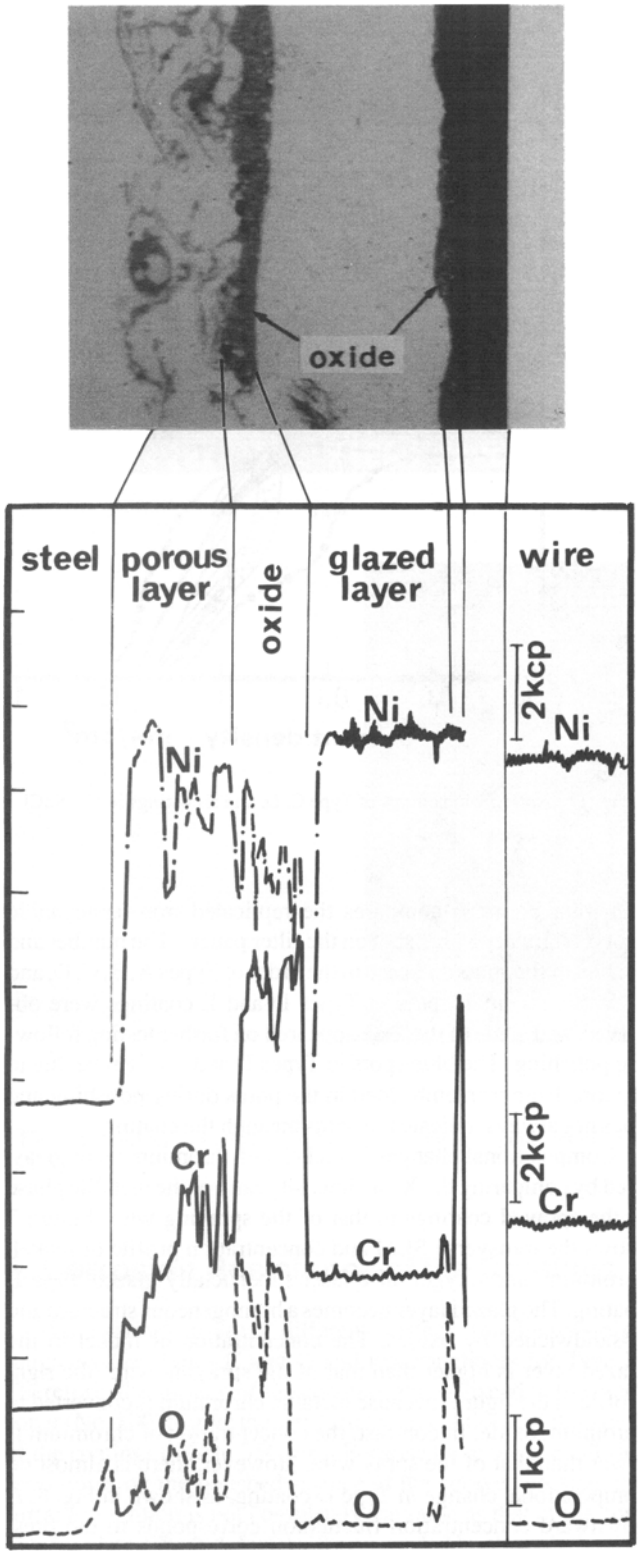

Fig. 7 Transverse SEM and characteristic X-ray profile of nickel, chromium, and oxygen in the Type B coating.

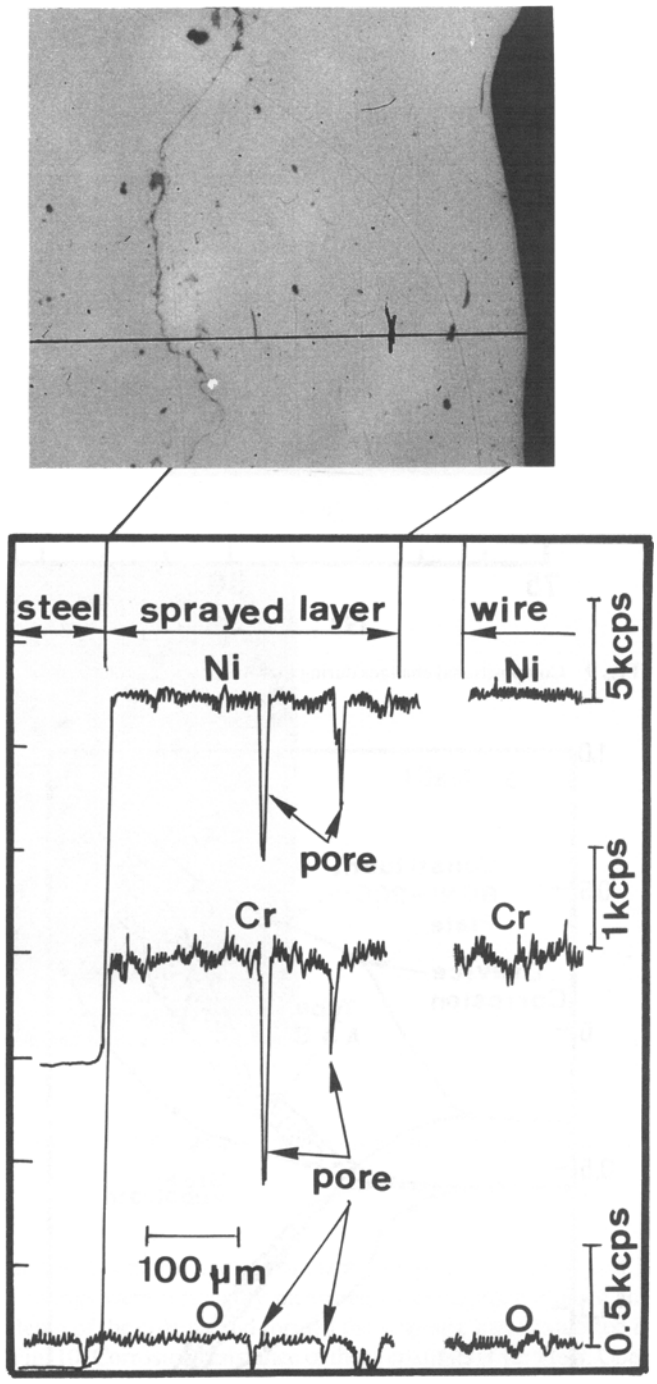

Fig. 8 Transverse SEM and characteristic X-ray profile of nickel, chromium, and oxygen in the Type D coating.

of oxides. The coating/substrate interface could not be observed on an unetched specimen. Type E, however, contains traces of oxides along the periphery of unmelted particles. This oxide originally is formed during preparation of the powder atomization because the powder is light brown-gray in color. The microstructural quality of the coatings improves in the order of Types A, B, C, E, and D. These results strongly indicate that the adoption of wire and arc spraying in an inert gas is essential for production of high-quality coatings and also that such coatings can be achieved by on-site spraying.

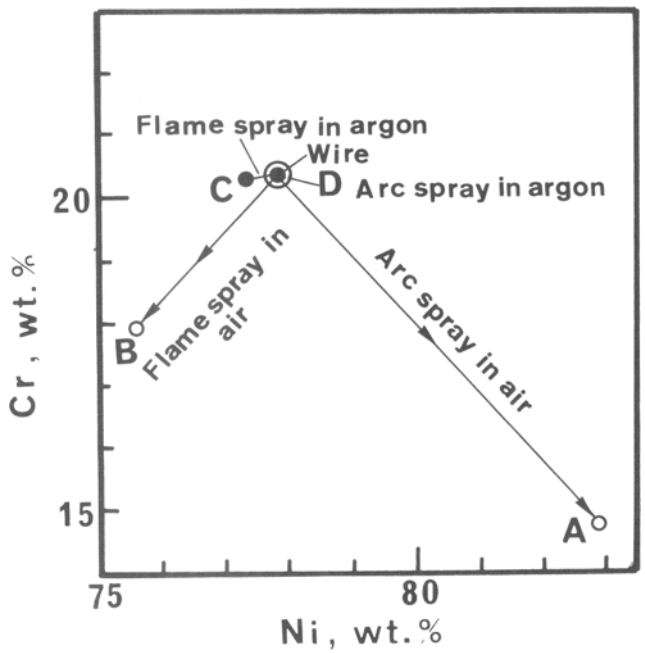

Fig. 9 Compositional changes during thermal spraying processes.

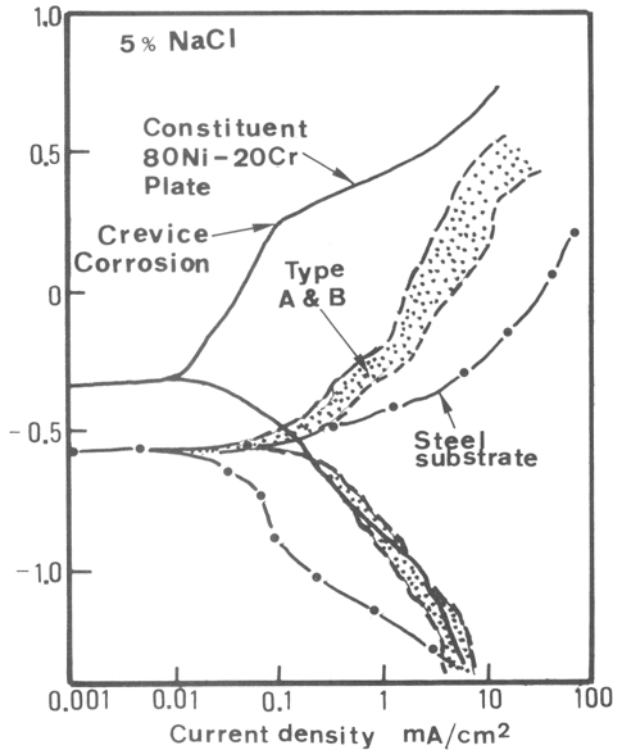

Fig. 10 Comparison of polarization curves of Type A and B coatings with those of constituent plate and substrate steel in 5% NaCl solution.

Connected paths through the coating were examined using the ferroxyl test according to the Japanese Industrial Standard JIS H 8666.[9] This test originally was developed to examine the paths through sprayed ceramic coatings; however, it can be applied to coatings studied in this work because they do not contain iron. Figure 6 compares the replicated iron-ferricyanide spots (originally a blue spot on the filter paper). The number and density of the spots decrease in the order of Types A, B, C, D, and E. Very few small spots in Types D and E coatings were observed, and some of these disappeared on further testing following polishing. The blue spots in Types D and E might be due to the ions from iron embedded in the pores during polishing and does not always indicate the paths through the coating.

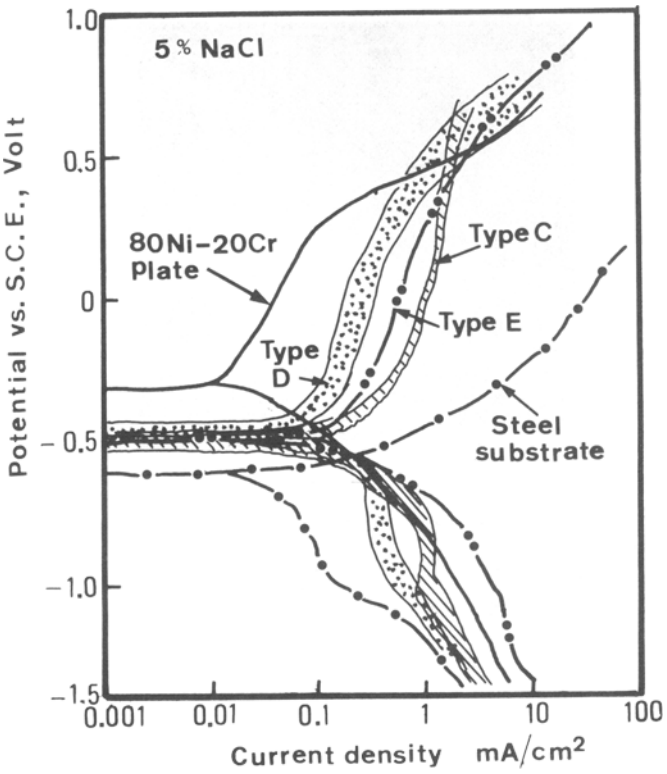

Fig. 11 Polarization curves of Type C, D, and E coatings in 5% NaCl solution.

Compositional changes in nickel and chromium were measured by comparing the X-ray intensity ratio of the metallic phase in the sprayed coatings to that of the spraying wire. Figure 7 shows the transverse SEM and concentration profile of nickel, chromium, and oxygen of a laser superficially glazed Type B coating. The glazed layer becomes a homogeneous structure and is sandwiched by oxides. The concentration of nickel in the glazed layer is higher than that of the spraying wire (the right profile in the figure) because metallic chromium is converted to chromium oxide. In contrast, the concentration of chromium is lower than that of the spray wire. However, there is almost no compositional change in Type D coating, as shown in Fig. 8. A downward concentration fluctuation corresponds to the presence of pores. The compositional change is summarized in Fig. 9. Large compositional changes occur in conventional spraying; however, this is minimized or eliminated in shrouded gas spray methods. Although the cost of spraying in argon gas is almost seven times that of conventional spraying, the arc spraying of wire in argon gas could produce high-quality coatings without oxides (Type D).

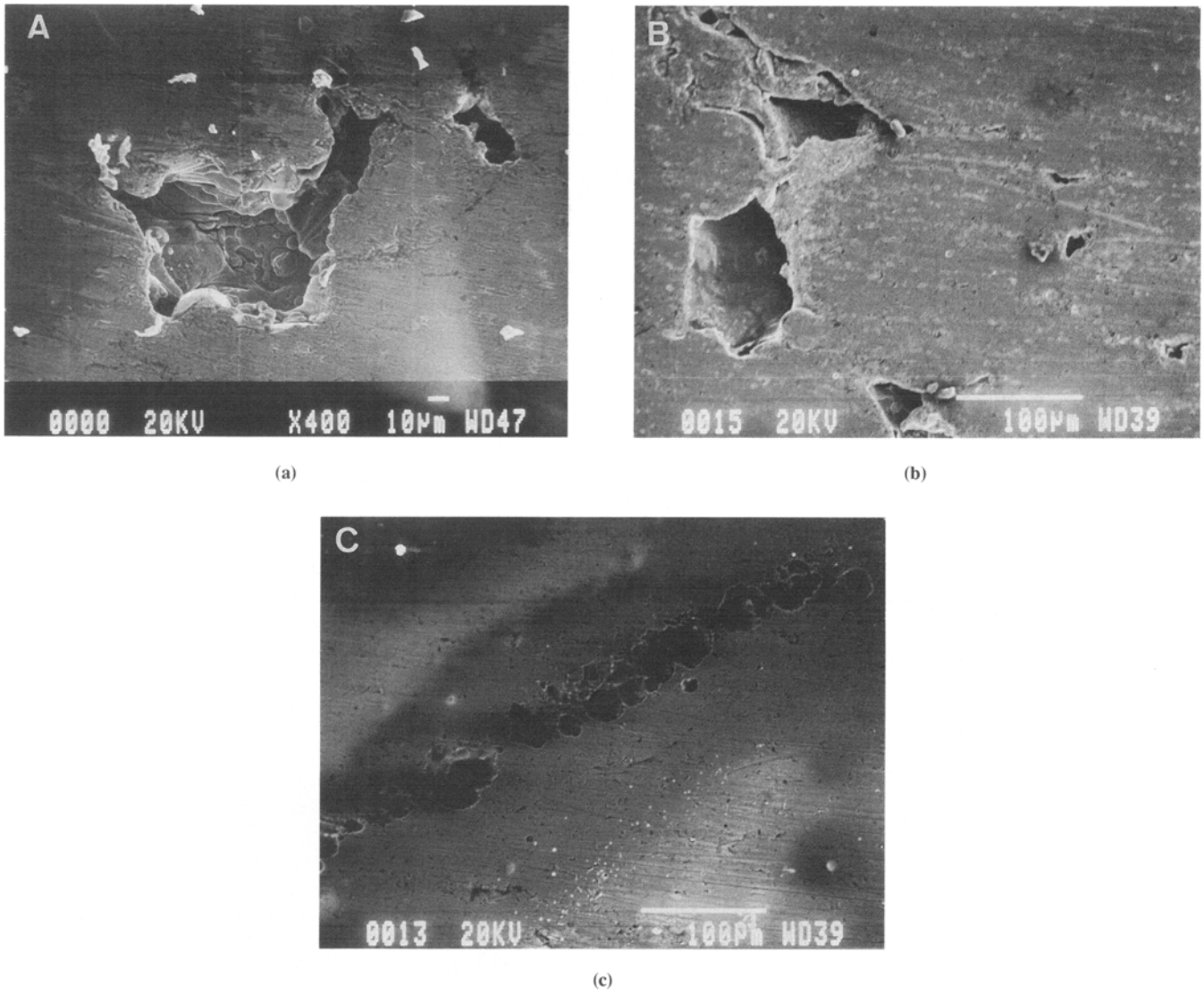

Fig. 12 Surface morphology of Type D coating after polarization in 5% NaCl solution. (a) Before polarization. (b) After polarization. (c) Beneath the O-ring.

4. Corrosion Resistance of the Coatings

The coatings possess different surface roughness—high roughness for Types C and D and low roughness for Type E. Therefore, the surface of the coatings was polished with emery paper (No. 800) to give the same surface condition and thickness of the coatings (400 to 350 µm). Because there were small isolated pores on the polished surface of the sprayed coating, the surface condition is not completely the same as that of the constituent plate. These defects will be revealed by the polarization curves.

4.1 *Corrosion Resistance in 5% NaCl Solution*

This corrodant was used for screening the corrosion resistance of the coatings. The coatings that passed this screening were submitted to further polarization measurements in sulfuric and hydrochloric acids. Polarization curves of Type A and B coatings were repeatedly measured by changing the place and depth of the coating and formed the response band exhibited in Fig. 10. Corrosion resistance of these coatings is very low. Open circuit potential of Types A and B is –0, 6V vs SCE (saturated calomel electrode) and the same as that of the substrate steel. This suggests that the corrodant penetrates the coatings and reaches the substrate steel. Current density at anodically polarized conditions is close to that of the substrate steel and is considered to be a limiting diffusion current of anodic dissolution rather than the passivation current density of 80Ni-20Cr alloy. Severe rusting on a coating that was exposed in air for 3 days after polarization was observed and indicates that these coatings could not be used as a protective coating against wet corrosion. Only one path through the coating is necessary for corrodant penetration, and this is deleterious for isolating the substrate from the environment. Furthermore, the coating of high nickel-

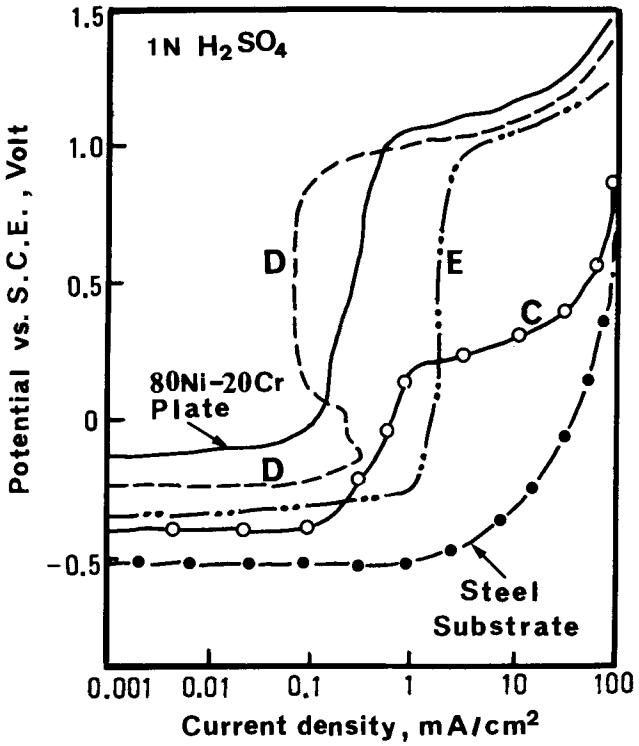

Fig. 13 Anodic polarization curves of Types C, D, and E coatings in 1*N* H_2SO_4 solution.

chromium alloy will accelerate the corrosion of the substrate steel when the corrodant impregnates the coating because the potential of steel is shifted to be more noble by galvanic coupling with nickel-chromium alloy.

Corrosion resistance of Types C, D, and E coatings are compared in Fig. 11. Corrosion resistance, in terms of the current density at anodically polarized potential, increased in the order of Type D, E, and C. This alloy is passivated when immersed in a 5% NaCl solution and, therefore, no clear Flade potential can be observed. The passivation holding current density of Type D coating is close to that of the constituent 80Ni-20Cr plate. The corrosion resistance of the Type D coating was improved almost a thousand times over the substrate steel based on the current density at a potential of 0 V vs SCE. The inferior corrosion resistance of the Type D coating to that of the constituent 80Ni-20Cr plate is due to pitting corrosion associated with isolated micropores and severe crevice corrosion beneath the O-ring, as shown in Fig. 12. However, the Type D coating that was exposed in air for 4 weeks after the polarization did not suffer any rusting. No attack of the substrate was revealed by metallographic examination.

4.2 *Corrosion Resistance in 1N Sulfuric Acid Solution*

Only three coatings (Types C, D, and E) were submitted to polarization measurements in 1*N* H_2SO_4 solution. The constituent plate shows passivation, as indicated in Fig. 13. The passivation potential (Flade potential) is not clear, because this alloy is in the passivated condition on being immersed. The Type D coating also shows passivation in a wide potential range. The critical passivation current density of the Type E coating is one order of magnitude higher than that of the Type D coating. This fact indicates that the arc spraying of wire in argon gas is able to produce a coating with corrosion resistance superior than that of the LPPS coating (Type E). The corrosion resistance of the Type C coating was not as high due to its inferior quality.

Figure 14 shows surface (a) and fracture surface (b) of the coating that is produced by mechanical impact in liquid nitrogen, and transverse SEM (c) of the Type D coating after being polarized for 2 h at the potential of –0.2 V vs SCE, at which the highest corrosion rate is observed. Attack progresses along the paths produced by the rapid solidification; however, the substrate is still sound. The corrosion resistance of the coating for long term use is not the same as that of the constituent alloy; however, its corrosion resistance is greatly improved by the adoption of a portable controlled atmosphere spraying system.

4.3 *Corrosion Resistance in 1N Hydrochloric Acid*

As shown in Fig. 15, the constituent plate undergoes severe crevice corrosion beneath the O-ring at potentials nobler than +0.25 V vs SCE. Polarization behavior of the Type D coating is very similar to that of the constituent plate. Severe crevice corrosion underneath the O-ring for the Type D coating was not observed. However, isolated attack (Fig. 16) similar to filiform corrosion was associated with the paths. No severe crevice corrosion of the Type D coating beneath the O-ring appears to closely correlate to the filiform-like attack. Potential paths might provide favorable places for crevice corrosion to take place. Corrosion potential and anodic current density are almost the same for Types C and E coatings and between the Type D coating and substrate.

Another interesting phenomena is the polarization curve of the Type C coating impregnated by an organic silicone sealant. The current density of this specimen at potentials more noble than +0.25 V is lower than that of the constituent 80Ni-20Cr plate. The fact that silicone sealing of the Type D coating does not improve the corrosion resistance means that the Type C coating possesses paths in which sealant impregnates; however, the Type D coating does not have those paths.

Use of both controlled atmosphere spraying and sealing is able to produce a coating with excellent resistance against wet corrosion. Further research on the corrosion protection mechanism of these coatings is required.

5. Conclusion

Two types of controlled atmosphere spraying systems, i.e., flame and DC arc spraying of wire in argon gas, were developed to deposit a corrosion-resistant coating. Characteristics and corrosion resistance of the 80Ni-20Cr coatings deposited on carbon steel by these methods were compared with that of coatings deposited by the conventional and low-pressure plasma spraying.

The results obtained are summarized as follows: The coatings deposited by conventional spraying contain a number of oxides and pores and permit the penetration of corrodant to the substrate. Porous coatings do not provide any corrosion resistance against corrosive environments in the as-sprayed condition.

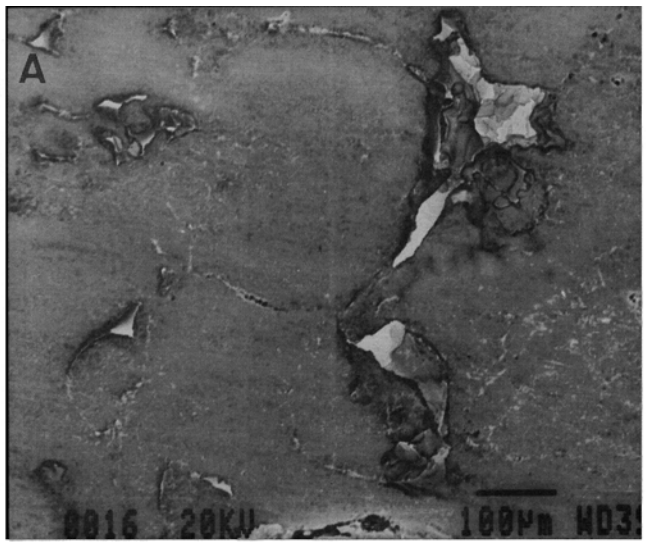

(a)

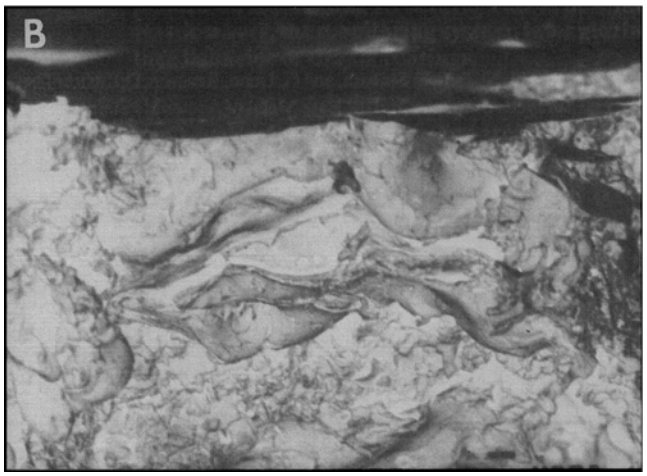

(b)

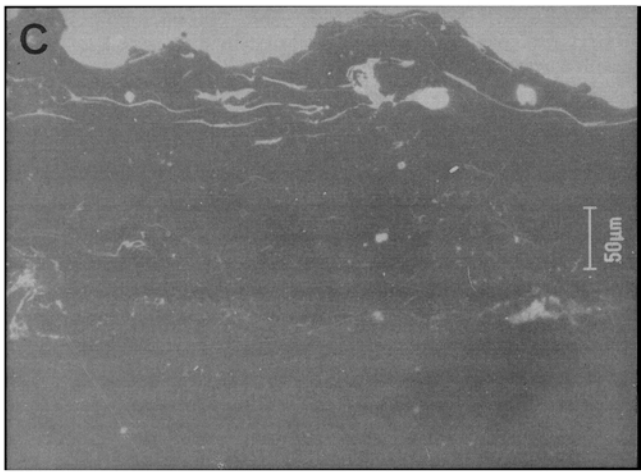

(c)

Fig. 14 Surface (a), fracture surface (b), and transverse photographs (c) of the Type D coating after being polarized for 4 h at –0.2 V vs SCE in 1*N* H_2SO_4 solution.

Coatings deposited by flame spraying of wire in argon gas and the low-pressure plasma spraying of powder contain small quantities of oxides and pores. On the other hand, arc spraying of wire in argon gas is able to produce high-quality coatings that are almost free of oxides and pores.

The coating deposited by arc spraying of wire in argon gas exhibits superior corrosion resistance to that of coatings deposited by low-pressure plasma spraying. The corrosion resistance of this coating is not the same as that of the constituent alloy because of the existence of isolated small pores and potential paths in the coating. Pitting and crevice corrosion associated with pores and paths gradually progresses in corrosive solutions.

Corrosion resistance of coatings deposited by flame spraying in argon gas was greatly improved by sealing with organic silicone compound, and sometimes, the corrosion resistance was higher than that of the constituent alloy.

Acknowledgment

This research was carried out under the financial support of the Nickel Development Institute (NiDI). The authors would like to express their sincere thanks to the NiDI.

References

1. T. Kato, H. Saito, M. Nakajima, and G. Ueno, Application of Thermal Sprayed Coating for Anti-Corrosion in Chemical Equipments, *Proc. Surf. Eng. Int. Conf.*, Japan Thermal Spraying Society, Tokyo, 1988, p 397-404
2. T. Sakaki, M. Kato, and G. Ueno, Application of Sprayed Cr-Ni Coating to Alkaline Plant, *Thermal Spraying Technol.*, Vol 9 (No. 4), 1990, p 72-77 (in Japanese)

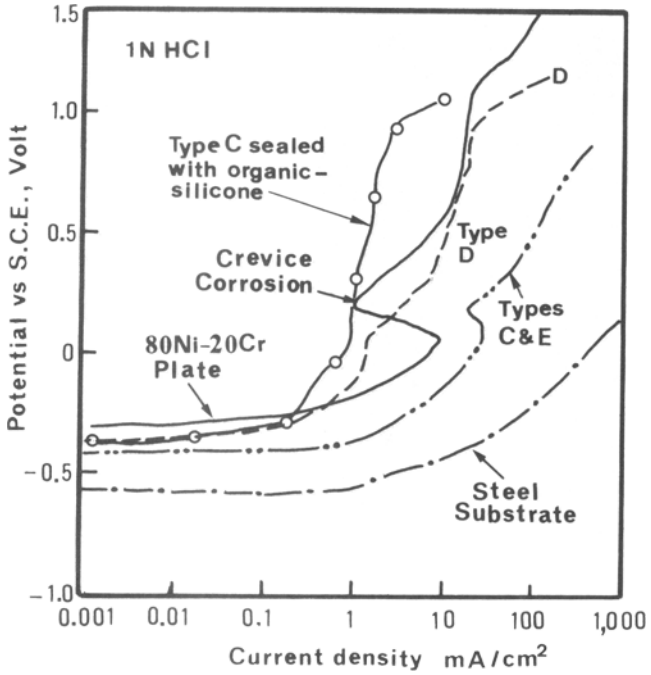

Fig. 15 Polarization curves of Type C, D, and E coatings in 1*N* HCl solution.

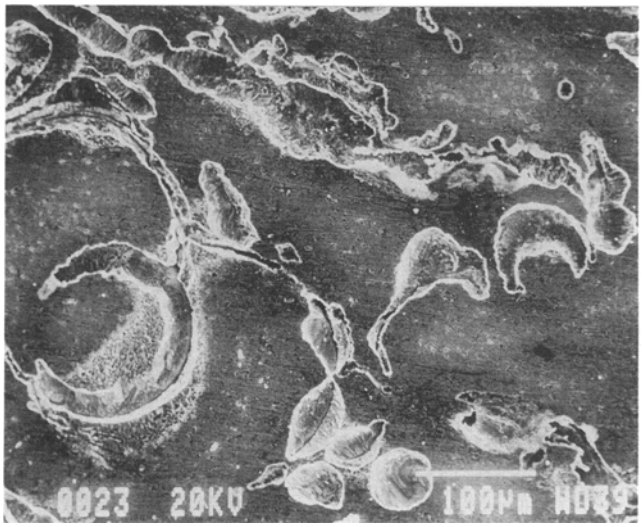

Fig. 16 Surface morphology of Type D coating after the polarization in 1*N* HCl solution.

3. M. Takemoto, Laser Surface Modification of Plasma Sprayed Oxide Ceramic Coat for Anti-Corrosion Performance, *High Power Laser*, Niku-Lari, Ed., Pergamon Press, Oxford, 1989, p 75-88
4. K. Hayashi, S. Kajiwara, K. Fujiwara, and M. Inaba, Damage and Consumption Process for Al-Zn Alloy Thermal Sprayed Coat of Open Rack Vaporizer, *Kobe Res. Develop.*, Vol 41 (No. 4), 1991, p 111-114
5. Y. Enami and M. Takemoto, Laser Treatment of Sprayed Ni-Cr Coat for Anti-Corrosion Performance, *Corros. Eng.*, Vol 39 (No. 8), 1990, p 416-424
6. K. Kamachi, N. Tani, T. Shibata, and G. Ueno, Reactive Diffusion Thermal Sprayed Aluminum and the Base Metal of Austenitic Stainless Steel and Its Effects on Cracking Behavior by Stress Corrosion Cracking, *Corros. Eng.*, Vol 39 (No. 3), 1990, p 113-118 (in Japanese)
7. M. Murakawa, S. Watanabe, and Y. Sugimoto, On Some Application of Thermal Sprayed Coating with HIP Post Treatment, *J. Jpn. Thermal Spraying Soc.*, Vol 25 (No. 3), 1988, p 18-26 (in Japanese)
8. Y. Longa and M. Takemoto, High Temperature Corrosion of Laser Glazed Alloys in Na_2SO_4-V_2O_5, *Corrosion*, Vol 48 (No. 7), 1992, p 599-607
9. Japanese Industrial Standard, "Testing Methods for Thermal Sprayed Ceramic Coatings," JIS H 8666, 1980